Characterization Method for Gas Flow Reactor Experiments - NH<inf>3</inf>Adsorption on Vanadium-Based SCR Catalysts

I&EC research
Industrial & Engineering Chemistry Research
pubs.acs.org/IECR
Article

Characterization Method for Gas Flow Reactor Experiments—NH_3 Adsorption on Vanadium-Based SCR Catalysts

Andres F. Suarez-Corredor,* Matthäus U. Bäbler, Louise Olsson, Magnus Skoglundh, and Björn Westerberg

Cite This: *Ind. Eng. Chem. Res.* 2021, 60, 11399−11411

Read Online

ACCESS | Metrics & More | Article Recommendations | Supporting Information

ABSTRACT: In this study, NH_3 adsorption isotherms for a commercial vanadium-based SCR catalyst coated on a monolith substrate were obtained using a gas flow reactor over a wide range of parameters which have not been performed before in a single study. The isotherms were obtained under different conditions, where adsorption temperature, NH_3 concentration, water concentration, washcoat loading, and catalyst oxidation state were varied. For this purpose, a systematic data processing method was developed, which characterizes the dispersion and delay effects in the experimental setup using a residence time distribution model, and artifacts such as NH_3 adsorbed in the experimental setup and uncertainties in the washcoat loading were removed. As a result, data from different catalyst samples were integrated, and adsorption isotherms with low data spread and well-defined regions were obtained. This allows the identification of the complex nature of the catalyst and dynamics, where multiple types of adsorption sites are present. For instance, the oxidized catalyst has 50% higher NH_3 storage capacity compared to the reduced state of the sample. Moreover, water reduces the NH_3 storage capacity at high concentrations (5.0%), whereas at low concentration (0.5%), water increases the NH_3 adsorption capacity for an oxidized catalyst. The proposed data processing method can be extended for the analysis of further phenomena in catalysts studied using gas flow reactors, complementing current methods and providing information for models with extended validity and lower parameter correlations.

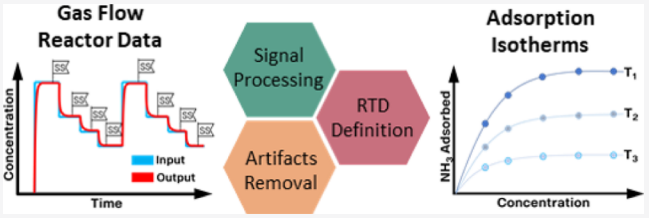

INTRODUCTION

The emission after-treatment system of an internal combustion engine plays an important role in reducing the environmental impact of the combustion technology.[1] Despite the current trend toward alternative drive trains, the internal combustion engine is expected to have a significant share also in the future power-train mix, at least in the medium term.[2] Current efforts to replace fossil fuels with biofuels or renewable synthetic fuels help to further reduce the negative impact of combustion engines.[3] In this regard, further development of after-treatment systems is a pressing issue and presents a challenging research task. Specifically, the development of after-treatment systems that fulfill current and future environmental regulations requires detailed experimental data over a wide parameter range, which in consequence calls for the development and improvement of experimental and theoretical techniques for understanding the nature of a catalyst.[4,5] Among the main experimental setups used for catalyst studies, gas flow reactors provide the flexibility to emulate conditions relevant for industrial applications, at a small but geometrically and structurally similar scale.[6,7]

In an emission after-treatment system, the selective catalytic reduction (SCR) unit reduces nitrogen oxides (NO_x) into N_2 and water using NH_3 from an aqueous urea solution.[6] The main SCR technologies used in automotive applications are currently based on vanadium oxide or copper-functionalized zeolites.[1] Although considered less modern, vanadium-based catalysts are still used since they provide high conversion and selectivity in a wide range of temperatures (300−450 °C) with resistance against sulfur and alkali poisoning.[8] The SCR reaction mechanism over vanadium-based catalysts involves multiple steps, including adsorption of NH_3 on the catalyst surface. Adsorption of NH_3 and the resulting NH_3 storage capacity are important features for the SCR catalyst as they determine the catalyst performance under transient conditions. Proper characterization of NH_3 adsorption provides improvements for reducing further emissions as the side reactions, and the NH_3 injection could be minimized.[9]

Adsorption of NH_3 is usually characterized by temperature-programmed desorption (TPD) experiments.[9−11] TPD allows for robust measurements of NH_3 at relatively small experimental effort. However, TPD experiments have some limitations for monolith samples. If the ramp speed is too high,

Received: April 19, 2021
Revised: July 2, 2021
Accepted: July 2, 2021
Published: July 19, 2021

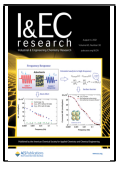

https://doi.org/10.1021/acs.iecr.1c01480
Ind. Eng. Chem. Res. 2021, 60, 11399−11411

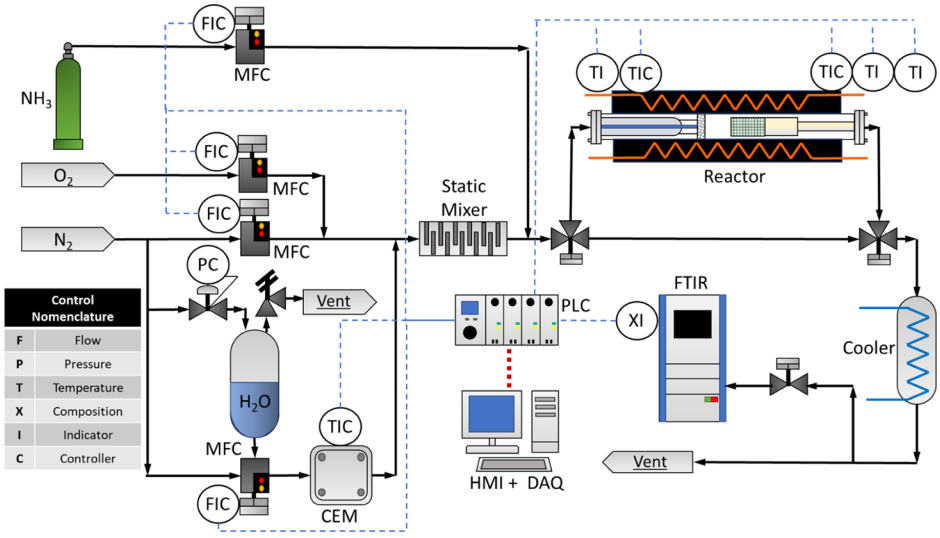

Figure 1. Experimental setup scheme.

difficulties may arise while ramping-up the temperature to reach equilibrium conditions and temperature gradients may be present in the monolith due to its thermal inertia. In addition, for samples with a thicker washcoat, mass transfer needs to be considered. Therefore, the information obtained from a TPD experiment for identifying multiple adsorption sites and interactions with other compounds such as water in industrial monolith samples is limited. In order to address these limitations, the present work aims to use a gas flow reactor for estimating the NH_3 adsorption isotherms in a wide experimental region.

Gas flow reactors are common setups in catalytic research, that is, they have been used to characterize reaction pathways for the standard SCR, fast SCR, NH_3 oxidation reaction, and so forth.[8−12] For instance, Olsson et al.[10,12] used a gas flow reactor to study the SCR reaction pathway over a Cu-ZSM-5 catalyst. They performed multiple experiments capturing the main features for the SCR mechanism based on which a detailed kinetic model was developed. Åberg et al.[13,14] proposed a methodology for parameter estimation for an SCR catalyst model using data from gas flow reactors. Their method is sequential, evaluating the impact on parameter fitting at each step and defining suitable simplifications for obtaining fast and reliable models. Their method is applied to different components in an after-treatment system such as SCR catalysts, diesel oxidation catalysts (DOC), diesel particle filters (DPF), and ammonia slip catalysts (ASC).[15]

Furthermore, gas flow reactors are also used as a validation tool when the intrinsic kinetics are determined from microreactor experiments with the catalyst in powder form, that is, instead of the monolith employed in the final application. Nova et al.[11] used this method to describe the inhibiting effect of NH_3 for the SCR reaction over vanadium-based catalysts at low temperature. The experiments included transient steps and temperature-programmed reaction. Tronconi et al.[8] developed a mathematical model to describe unsteady SCR processes over a full-scale vanadium-based catalyst. Apart from the validation in a gas flow reactor, they compared their model to full-scale data from engine bench tests. Chatterjee et al.[9] used data obtained from a microreactor to develop a 2-D model for a vanadium-based SCR catalyst with application to coated and extruded monoliths. The estimation of mass and heat transfer parameters was performed using gas flow reactor data, obtained from nonsteady experiments with stepwise concentration changes in the feed using fast response pulses. Ciardelli et al.[16] used a similar method for studying the kinetics for NH_3 adsorption and desorption on a vanadium-based SCR catalyst. Considering a wide range of experimental conditions, the authors propose different reaction mechanisms at low and high temperatures. Their models show adequate agreement with experimental data with some deviations for NH_3 adsorption under transient conditions.

The present work aims at using a gas flow reactor for measuring NH_3 adsorption on a commercial vanadium-based SCR catalyst, with TiO_2 as a support, coated on a monolith substrate. A wide range of experimental conditions are considered in terms of NH_3 concentration, adsorption temperature, water concentration, catalyst oxidation state, and washcoat loading. For this purpose, an experimental procedure is developed that allows for estimating the NH_3 adsorption from the step response of a change in the feed concentration of NH_3 to the reactor. A calibration procedure and a data processing method are proposed where the experimental setup is characterized as a real reactor by means of its residence time distribution (RTD). The data processing method allows for the identification and the systematic removal of experimental artifacts, enabling efficient and robust measurements of adsorption isotherms with high confidence. The proposed method demands less resources and provides a characterization for transient data compared to static compensation methods such as baseline subtraction where experiments are performed without a catalyst sample and the obtained signal is subtracted from the actual experiment signal. With respect to the TPD method, the proposed work assures equilibrium throughout the desorption steps and it allows the observation of the influence of the catalyst state on the NH_3 storage capacity. Furthermore, this method provides quantification of artifacts, relevant for experimental design. The adsorption data presented in this work cover a wide region of conditions, thus extending available adsorption data, which enables future development of adsorption and SCR catalyst models with a wider range of applicability.

https://doi.org/10.1021/acs.iecr.1c01480
Ind. Eng. Chem. Res. 2021, 60, 11399−11411

METHODOLOGY

The NH_3 adsorption experiments were carried out in a gas flow reactor designed for studying monolith catalyst samples. Figure 1 shows a scheme with the main components of the experimental setup. It can be divided into three sections: flow conditioning, reactor and flow analysis. In the flow conditioning section, the gas flow and composition are adjusted by the use of mass flow controllers (MFCs). In the reactor section, the monolith sample is placed and the temperature is controlled. Finally, in the flow analysis section, a Fourier transform infrared spectroscopy (FTIR) equipment analyzes the composition from the reactor. All the equipment is connected by stainless-steel piping which is heated to 180 °C in order to minimize unwanted adsorption and to ensure that water remains in the vapor phase. The main components of the experimental setup are described in Table 1.

Table 1. Experimental Setup Main Components

component	reference	principle/function
MFC	Bronkhorst EL-FLOW select	flow is measured and controlled based on the thermal mass flow principle
CEM module	Bronkhorst	water and N_2 are mixed and heated to ensure water vapor flow
Coriolis flow meter	Bronkhorst MINI-CORIFLOW-M13	water flow is measured and controlled based on Coriolis principle
Thermocouples	Type K class 1	change of voltage due to thermoelectric effect
FTIR	AVL Sesam i60 FT	FTIR, for measuring gasconcentration
O_2 sensor	Magnos 106 O_2 sensor	paramagnetic sensor
HMI and DAQ	ProControl Dizanta Suite + MatLab	Human Machine Interface for control and Data Adquisition tool

The experimental setup uses N_2 as a carrier gas. Two NH_3 gas bottles with different concentrations were used and supplied by Air Liquide: 3.6% for adsorption experiments at 75 ppm or higher NH_3 concentrations and 1.0% for concentrations lower than 75 ppm. The different gas bottle concentrations were used to operate the MFC in the operating range where the highest precision is achieved. The reactor zone is divided into different regions: the preheating region, where the flow is heated to a specified temperature and stabilized, and the reaction zone, where the sample holder for the catalyst sample is located. Each region has its own temperature controller, and in the preheating region, a cascade control loop is used. Four thermocouples are located in strategic locations to monitor and control temperature, before, after, and in the sample, ensuring isothermal conditions. A scheme of the reactor zone is presented in Figure 2.

NH_3 Adsorption Experiments. NH_3 adsorption experiments were performed in the gas flow reactor setup for the state-of-the-art vanadium-based SCR catalyst with TiO_2 as a support supplied by Umicore. Three samples, described in Table 2, with the same formulation but different nominal washcoat loadings (given by the supplier) were used. The actual washcoat loading is also included in the table, estimated from the proposed method, and described in the Washcoat Uncertainties section. The total volume for the samples also differed. The low-volume sample was used to perform NH_3 adsorption experiments at low concentration since an NH_3 gas bottle at low concentration (1.0%) was needed to employ the MFC in an optimal accuracy region.

The catalyst samples were installed in the sample holder in the reactor section and a ceramic cloth was placed around to fixate the sample and to avoid gas bypassing. Then, the thermocouples were located in the defined locations in the sample. After the sample was installed, a leak detection procedure was performed to confirm that the system was properly sealed and connected. This procedure involves increasing the pressure in the experimental setup and switching the three-way valves located in the reactor section, directing the flow through the bypass and isolating the reaction zone. If the sample was properly installed, the pressure in the reactor should be maintained. For each experiment, the FTIR equipment was calibrated, defining the baseline signal with

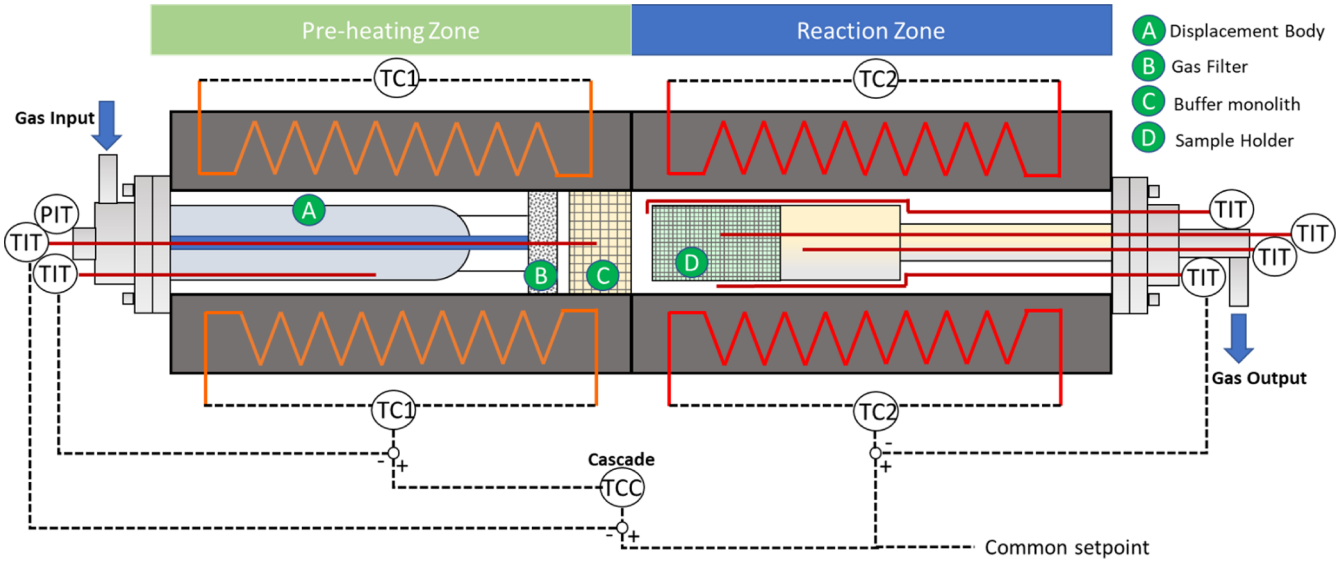

Figure 2. Reactor schematic. The black dashed line represents the cascade control scheme between the two reactor zones, where TIT is a temperature transmitter and TC is a temperature control element.

https://doi.org/10.1021/acs.iecr.1c01480
Ind. Eng. Chem. Res. 2021, 60, 11399−11411

Table 2. Main Catalyst Sample Parameters

ID	type	length (cm)	diameter (cm)	weight (g)	nominal washcoat loading (g/L)	actual washcoat loading (g/L)
HC-LL	high concentration, low loading	7.64	2.43	20.67	288	284
HC-HL	high concentration, high loading	7.68	2.48	23.77	371	383
LC-LL	low concentration, low loading	2.66	2.52	7.15	288	301

only N_2 being present. The calibration was performed using the built-in protocol in the equipment.

The samples were degreened before the experiment. The degreening procedure is presented in Table 3. The main objective of this procedure is to stabilize the catalyst performance by cleaning the catalytic surface from adsorbates. The degreening procedure was run until two subsequent SCR activity steps gave the same NO_x conversion. If not, the stabilizing step was repeated.

Table 3. Sample Degreening Steps for the Catalyst Samples

procedure	step	flow (NL/min)	temp. (°C)	composition	time (min)
Degreening	purging	30	450	5% H_2O	5
	SCR activity	30	450	500 ppm NO, 500 ppm NH_3, 5% H_2O	5
	stabilizing	30	450	5% H_2O, 5% O_2	10, 20, 60
	final purging	30	450	N_2 only	5
	oxidizing	30	450	5% O_2	20

After degreening, a pretreatment step was performed to set the oxidation state for the sample. Two different procedures for pretreatment were employed to reach the desired oxidation state of the catalyst sample, namely, a reduced state and an oxidized state. Each treatment is explained in Table 4.

Table 4. Sample Pretreatment Steps for Defining the Catalyst Oxidation State

catalyst state	step	flow (NL/min)	temp. (°C)	composition	time (min)
oxidized state	purging	50	500	N_2 only	3
	oxidizing	50	500	5% O_2	10
	purging	50	500	N_2 only	3
reduced state	purging	50	500	N_2 only	3
	oxidizing	50	500	5% O_2	10
	purging	50	500	N_2 only	3
	reduction	50	500	500 ppm NH_3	20
	purging	50	500	N_2 only	3

Then, the temperature is set to the experiment temperature and the NH_3 adsorption experiment is started. The experiment is initiated with an adsorption step with high NH_3 concentration (1000 ppm for the high-concentration test and 150 ppm for the low-concentration test). Notice that this first adsorption step does not need to reach equilibrium since the accumulation is calculated based on constantly measuring the inlet and outlet NH_3 concentration and the proposed data processing method. Then, different steady-state desorption steps were reached by different NH_3 gas concentrations. The desorption steps were performed from high-to-low NH_3 gas concentrations: 450−75 ppm for the high-concentration test and 75−30 ppm for the-low concentration test, as presented in Figure 3. The adsorption and desorption sequence was repeated twice for repeatability purposes to increase the confidence in the obtained values and to help defining reference values for the flow calibration required in the data processing. The NH_3 adsorption experiments were repeated with 1-year difference in the same experimental setup with some modifications aimed to improve flow and heat distribution in the reactor zone. The high repeatability and low dispersion of the data validate the proposed method since the reactor characterization was replicated for both setups (before and after modifications). The pretreatment step (see Table 4) was repeated before each new NH_3 adsorption experiment at a new temperature. This process was repeated at different catalyst oxidation states and three different water concentrations: 0, 0.5, and 5%. The total volume flow for the overall experiment was set at 50 NL/min providing a gas hourly space velocity (GHSV) between 80,000 and 84,000 h^{-1} for the larger cores and 225,000 h^{-1} for the smaller core used at low-concentration measurements.

Moreover, for the experiments with the oxidized catalyst, the highest adsorption temperature used was 250 °C, as significant NH_3 oxidation could be observed at higher temperatures. For the reduced catalyst, the highest adsorption temperature was 400 °C. At higher temperatures, no significant amount of NH_3 is adsorbed on the vanadium-based catalyst. The overall experiment is described in Figure 3, with the panel (b) showing the step changes in the NH_3 concentration used to characterize the adsorption at a given temperature.

Data Processing. *Adsorption of NH_3.* Each experiment provides two signals, that is, the flow rate of NH_3 obtained from the MFC at the reactor inlet (hereafter denoted by q_{MFC}) and the mole fraction concentration of NH_3 obtained from the FTIR at the reactor outlet (hereafter denoted by y_{FTIR}). Both signals are in the form of discrete time series recorded at synchronized time intervals of $\Delta t = 1$ s. In order to use these two signals for the characterization of the NH_3 adsorption, we first applied a data processing procedure to adjust and convert the signals, as illustrated in Figure 4.

The data refining procedure consists of three steps. At first, an offset correction is applied to the FTIR signal (y_{FTIR}), since the zero value from the FTIR is not usually set at zero but to a closer value. The offset is calculated from the initial part of the experiment where no NH_3 is fed and it is subtracted from the original FTIR signal. Then, since the adsorption isotherm is built from estimating the NH_3 accumulation at each step of the step-change experiment, the identification of each individual step in the time series is required. This is done by analyzing q_{MFC} since it has less noise and the steps are well-defined. The proposed method consists of tracking the local derivative and defining a threshold based on the standard deviation of the measured derivative. A new step begins whenever the derivative of q_{MFC} exceeds the threshold value. Finally, the MFC flow signal (q_{MFC}) is converted to concentration (y_{MFC}). This is performed through the identification of common

https://doi.org/10.1021/acs.iecr.1c01480
Ind. Eng. Chem. Res. 2021, 60, 11399−11411

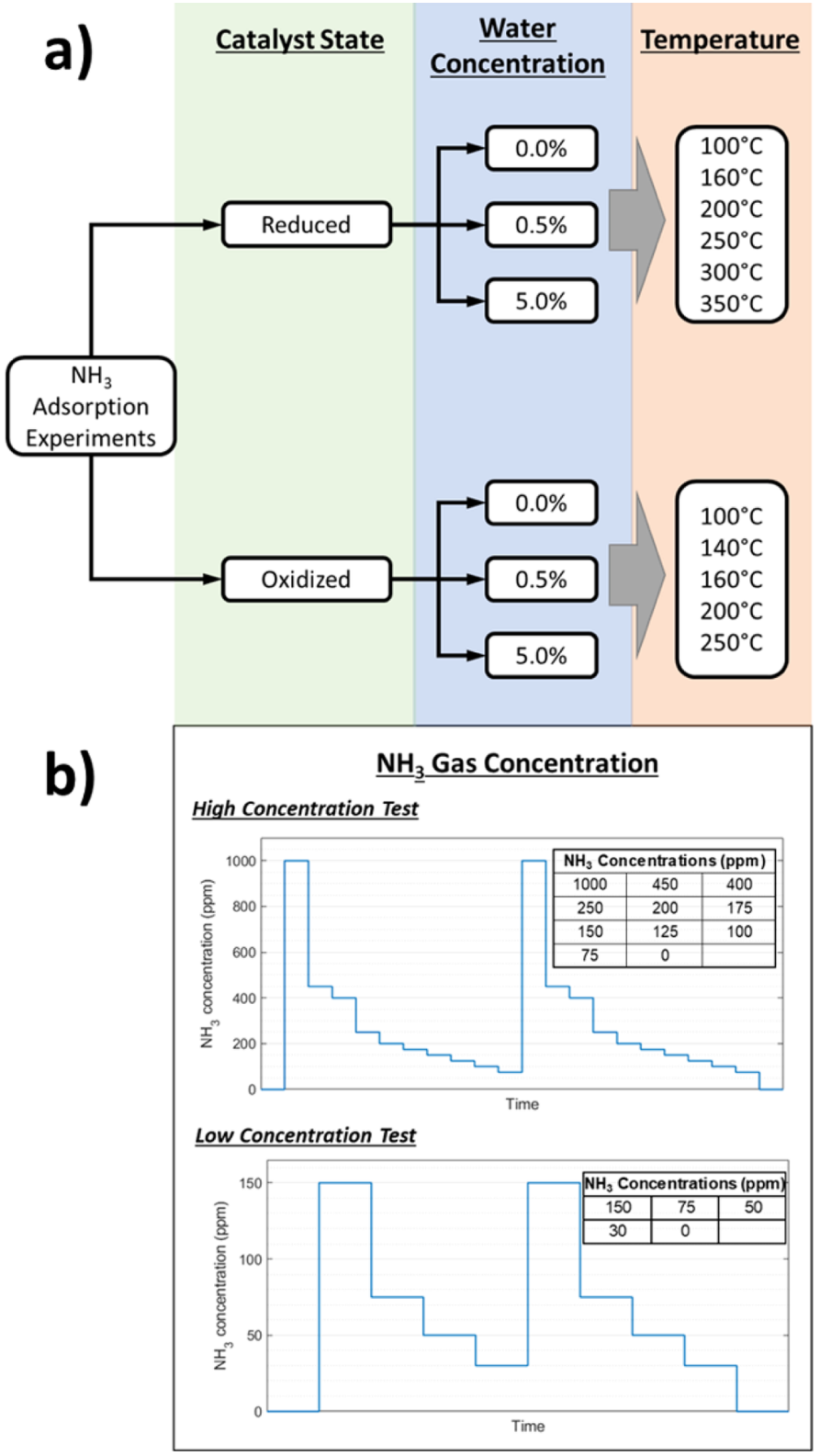

Figure 3. NH_3 adsorption experiments, (a) conditions for the catalyst state, water concentration, and temperature and (b) NH_3 concentration step sequence for high-concentration and low-concentration experiments. The NH_3 gas concentrations defining the adsorption/desorption steps are presented in the tables inside the figure.

steady-state points for all the experiments, that is, points where the FTIR signal corresponds to the feed rate of the MFC. Based on these points, a calibration curve is constructed using simple least square regression. Fine-tuning is then applied by minimizing the difference between the first and the second realization of three reference steps (in the step experiment, each step is repeated twice). Even if the composition could be calculated by the ideal gas law, using the FTIR measurements

https://doi.org/10.1021/acs.iecr.1c01480
Ind. Eng. Chem. Res. 2021, 60, 11399−11411

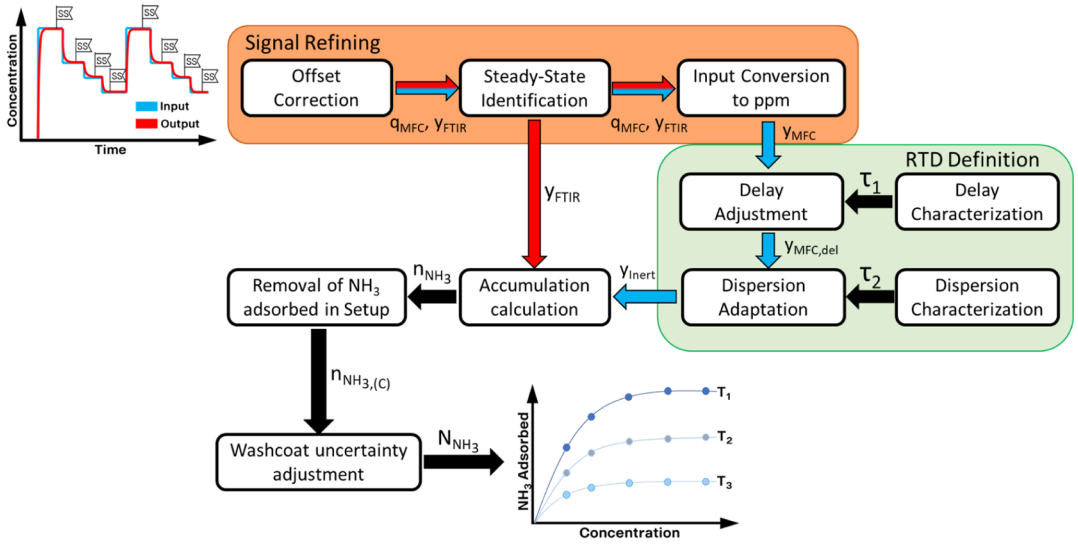

Figure 4. Data processing proposed method. In the figure, y_{FTIR} is the output signal from FTIR in ppm; q_{MFC} is the input signal from the NH_3 MFC in NL/min; y_{MFC} is the input signal converted to ppm; τ_1 and τ_2 are the time scale parameters for the delay and dispersion effects, respectively; $y_{MFC,del}$ is the input signal shifted in time due to delay effects; y_{inert} is the modeled inert tracer; n_{NH_3} is the NH_3 accumulated in the experiment; and $n_{NH_3,(c)}$ is the NH_3 accumulated in the catalyst sample after the amount adsorbed in the experimental setup is removed. N_{NH_3} is the normalized NH_3 accumulation by the washcoat loading.

is a more realistic approach for doing the flow conversion, since it accounts for the uncertainties in the experimental setup presented in the FTIR, MFCs, and gas bottle composition.

The data refining procedure delivers the converted input signal y_{MFC} and the offset-corrected output signal y_{FTIR} for each individual step of the experiment. Figure 5a shows these two signals for an experiment that included five steps. From the refined signals, the total amount of NH_3 adsorbed on the catalyst sample is obtained as

$$n_{NH_3} = F_{total}\int_0^{t_{int}} (y_{inert} - y_{FTIR})dt \quad (1)$$

where n_{NH_3} is the total amount of adsorbate, F_{total} is the total gas molar flow, t_{int} is the duration of the step, and y_{inert} is the concentration at the reactor outlet for an inert tracer gas. The latter is obtained from the input signal (y_{MFC}) and the RTD of the reactor through the following convolution operation

$$y_{inert}(t) = \int_0^t E(t')y_{MFC}(t - t')dt' \quad (2)$$

where $E(t)$ is the RTD of the reactor setup, which is modeled as the combination of a delay element and a dispersion element connected in series, as shown in Figure 6.[17,18] In other words, the RTD is formulated as a two-parameter model assuming that the flow pattern in the reactor can be approximated using a plug flow reactor (PFR) and a continuously stirred tank reactor (CSTR) in series. The resulting RTD model reads as

$$E(t) = \begin{cases} 0, & t < \tau_1 \\ \frac{1}{\tau_2} e^{-(t-\tau_1)/\tau_2}, & t \geq \tau_1 \end{cases} \quad (3)$$

where τ_1 and τ_2 are the time scale parameter for the delay element and the dispersion element, respectively (i.e., the PFR and the CSTR, respectively). Modeling $E(t)$ through a delay and a dispersion element is motivated as follows. If no reaction

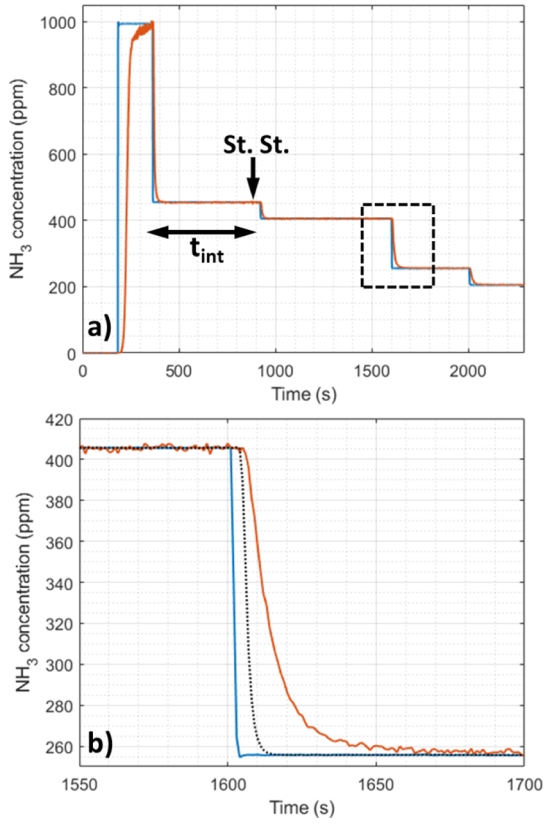

Figure 5. Signal refining and data processing of the step experiments. (a) Refined input signal (y_{MFC}, blue curve) and output signal (y_{FTIR}, red curve) for an experiment with five steps. t_{int} indicates the duration of a step and St.St. indicates the steady-state conditions established at the end of each step. (b) Close up of the third step from panel (a) including the convoluted input signal (y_{inert}, black dashed line).

or interactions are present in the reactor and a step input is fed, the output signal from the tracer will be shifted in time since

https://doi.org/10.1021/acs.iecr.1c01480
Ind. Eng. Chem. Res. 2021, 60, 11399−11411

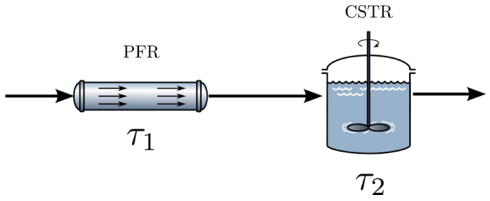

Figure 6. Reactor configuration for modeling the RTD. The time scale parameter τ_1 accounts for the delay effects, and the time scale parameter τ_2 accounts for the dispersion effects.

there is a delay as a result of the experimental setup volume, which the tracer will need to travel before reaching the outlet sensor, for example, FTIR. In addition, the sharp step used as an input will be smoothed due to the axial dispersion caused by diffusion.

The two time scale parameters in eq 3 were determined through independent experiments that considered a wide range of operation conditions. The delay time τ_1 was determined using CO_2. This gas shows minimal interaction with the experimental setup and therefore can be considered a tracer gas. Using CO_2 in step-input experiments allowed for including the characteristics of the FTIR into the delay time measurements (sensor response and internal signal processing might cause an additional delay). Measurements at different gas flow rates, reactor temperatures, MFC locations, and outlet measurement device (FTIR) were performed. Based on these measurements, a data-driven model was developed that allowed for expressing the delay time τ_1 as a function of the reactor configuration and the operation conditions.[19,20] The dispersion time scale τ_2 was determined using CO at high temperature as an inert gas, following the same concentration steps as in the NH_3 experiments. The determination of τ_2 from these experiments follows the same procedure as the one used for calculating y_{inert} outlined in Supporting Information. A detailed description on the procedure for determining τ_1 and τ_2 is given in Supporting Information.

With τ_1 and τ_2 at hand, the reactor outlet for a tracer gas follows eq 2. The convolution operation described by eq 2 was implemented in two steps. First, the converted MFC signal y_{MFC} was shifted in time by a time span τ_1. To keep the synchronized time at which the data was collected, the time-shifted MFC signal, $y_{MFC(del)}$, is obtained by interpolating between the data points of the original MFC signal, that is

$$y_{MFC(del,i)} = y_{MFC(i-a)} + \frac{y_{MFC(i-a+1)} - y_{MFC(i-a)}}{\Delta t}(a\Delta t - \tau_1) \quad (4)$$

where $a = \lceil \tau_1/\Delta t \rceil$, with $\lceil\rceil$ denoting rounding up to the next integer. In a second step, the time-shifted signal is subjected to the dispersion element, that is, the time-shifted signal is convoluted by e^{-t/τ_2}. As shown in Supporting Information, convolution with an exponential function is equivalent to applying a low-pass filter that processes the signals in an iterative manner, that is

$$y_{inert(1)} = y_{MFC(del,1)} \quad (5a)$$

$$y_{inert(i)} = f_{dis} y_{inert(i-1)} + (1 - f_{dis}) y_{MFC(del,i)} \quad (5b)$$

where $f_{dis} = e^{-\Delta t/\tau_2}$ is the smoothing factor. Figure 5b shows the input signal y_{MFC} (blue solid line) and its convolution y_{inert} (dashed line) together with the output signal y_{FTIR} (red solid line) for a single step of a representative experiment. The area segment between the red curve (y_{FTIR}) and the dashed curve (y_{inert}) is proportional to the total amount of NH_3 adsorbed onto the catalyst sample, as described by eq 1. The latter gives the adsorbed amount of NH_3 in units of moles. The total flow rate F_{total} appearing as a prefactor in eq 1 is obtained from the total volumetric flow supplied to the reactor and the ideal gas law as

$$F_{total} = \frac{q_{total}}{60}\frac{P_{ref}}{RT_{ref}} \quad (6)$$

where q_{total} is the total volumetric flow rate obtained from the MFCs at the reactor inlet, R is the ideal gas constant, and P_{ref} and T_{ref} are the reference pressure (101.325 kPa) and the reference temperature (273.15 K), respectively, at which the MFCs were calibrated.

The procedure described by eq 1 to eq 6 is applied to each concentration step of each experiment. Each of these steps represents an equilibrium state, affected by temperature, NH_3 gas concentration, H_2O gas concentration, and catalyst

Table 5. Model for Adsorption on the Experimental Setup[a]

site one:	site one:
$S_1 + NH_3 \rightleftharpoons S_1[NH_3]$	$n_{NH_3(1,exp)} = \frac{N_1 K_{11} C_{NH_3}}{1 + K_{11} C_{NH_3}}$
site two:	site two:
$S_2 + NH_3 \rightleftharpoons S_2[NH_3]$	$n_{NH_3(2,exp)} = N_2(\theta_{2A} + \theta_{2B})$
$S_2 + H_2O \rightleftharpoons S_2[H_2O]$	$\theta_{2A} = \frac{K_{21} C_{NH_3}}{1 + K_{21} C_{NH_3} + K_{22} C_{H_2O} + K_{22} K_{23} C_{NH_3} C_{H_2O}}$
$S_2{-}H_2O + NH_3 \rightarrow S_2{-}H_2O[NH_3]$	$\theta_{2B} = \frac{K_{22} K_{23} C_{NH_3} C_{H_2O}}{1 + K_{21} C_{NH_3} + K_{22} C_{H_2O} + K_{22} K_{23} C_{NH_3} C_{H_2O}}$
	$K_{2i} = A_{2i} \exp\left(\frac{-E_{2i}}{RT}\right)$
	total NH_3 adsorbed in the setup:
	$n_{NH_3(exp)} = n_{NH_3(1,exp)} + n_{NH_3(2,exp)}$

[a]The adsorption model assumes two sites, S_1 and S_2, on which NH_3 and H_2O adsorb. N_1 and N_2 describe the number of adsorption sites, $\theta_{2,AB}$ is the surface coverage of site 2 and the K_{ij}'s are adsorption equilibrium constants.

https://doi.org/10.1021/acs.iecr.1c01480
Ind. Eng. Chem. Res. 2021, 60, 11399−11411

oxidation state. Hence, each step presents a data point on the adsorption isotherm for NH_3.

Adsorption in the Experimental Setup. NH_3 and H_2O can adsorb on several surfaces such as stainless steel, present in pipes and accessories. This can distort the measurements of NH_3 adsorption on the catalyst sample. Therefore, it is necessary to measure this effect and remove the amount adsorbed by the experimental setup from the total calculated amount.[11] This was done by running a series of step-input experiments without the catalyst sample in the reactor. The absolute amount of NH_3 adsorbed in the setup was determined using the same data processing method. Due to the transient behavior between the steady-state desorption states, such an approach is suitable compared to, for example, static compensation methods where the signal from an experiment without the catalyst sample in the reactor is subtracted from the signal of the actual experiment.

For describing the amount of NH_3 that adsorbs in the empty reactor, a mechanistic Langmuir adsorption model was developed. The proposed model involves two sites (a single-site model site was tried but the results were deficient): site S_1 which is temperature-independent and assigned to the pipelines which are kept at constant temperature (180 °C) and site S_2 which is temperature-dependent and assigned to the reactor zone. Water has a temperature dependency and this effect was assigned to site S_2. The two-site model for adsorption in the experimental setup is summarized in Table 5. A genetic algorithm method was built to optimize the model parameters to the experimental data. The algorithm was initialized by empirical values for molecular adsorption.[21]

A total of nine parameters were fitted for describing NH_3 adsorption in the experimental setup. Notice that the adsorption model used here was used solely for parametrizing the measured adsorption in a sound framework. Confidence intervals and cross-correlation between parameters (and whether the data could have been described with fewer parameters) therefore were not explored.

With the proposed adsorption model at hand, it is possible to estimate the NH_3 adsorbed in the experimental setup ($n_{NH_3(exp)}$) for the actual temperature and NH_3 and water concentration. The calculated adsorbed amount in the setup is then subtracted from the total amount of adsorbed NH_3 in the reactor, that is

$$n_{NH_3(c)} = n_{NH_3} - n_{NH_3(exp)} \tag{7}$$

where $n_{NH_3(c)}$ is the NH_3 adsorbed over the catalyst sample, n_{NH_3} is the NH_3 adsorbed over the experimental setup and the catalyst sample, and $n_{NH_3(exp)}$ is the NH_3 adsorbed over the experimental setup without the catalyst sample estimated using the proposed model.

Washcoat Uncertainties. The amount of adsorbate on a monolith catalyst is typically reported as the amount of adsorbed NH_3 per surface area, mass, or volume of catalyst.[9,10,15] However, in order to compare different catalyst samples, it is meaningful to normalize the amount of adsorbate with the washcoat loading which requires an accurate estimation. In this study, two different washcoat loadings and two different catalyst sample sizes were used, as shown in Table 2. The normalized amount of adsorbed NH_3 was calculated from

$$N_{NH_3} = \frac{n_{NH_3(c)}}{\rho_{WC} V_s} \tag{8}$$

where $n_{NH_3(c)}$ is the amount of adsorbed NH_3 obtained from eq 7, ρ_{WC} is the catalyst washcoat loading in [g/L], and V_s is the sample volume in [L].

Using eq 8 with the nominal washcoat loading provided by the vendor (see Table 2), we observed minor differences when comparing different samples under the same conditions, making the adsorption isotherm curve not continuous. This can reduce the fitting performance when developing models. The difference could be explained by the uncertainty in the washcoat loading since deviations within a margin from the nominal value exist due to the nature of the complex catalyst manufacture process.[22] Moreover, the washcoat loading difference was noticed from visual inspection and weight difference between the samples with the same nominal washcoat loading. As a result, the nominal values for the washcoat loading can vary between certain margins. In an industrial sample, the washcoat loading is difficult to estimate by gravimetric methods since the discrimination between the uncertainties associated to the substrate and the washcoat is not possible. Besides, we aim to study the supplier sample preserving its integrity and properties for its use in the automotive industry. For these reasons, to account for the deviations in washcoat loading, a linear optimization method was developed to find the washcoat loading of each sample that minimizes the differences of the normalized adsorbate concentration (N_{NH_3}) from the different samples under certain reference conditions.[20] For the three samples involved in the tests for low and high concentrations, the reference point is set at 75 ppm since all the experiments included this NH_3 concentration. In addition, 200 and 250 ppm were also used as reference points for the high-concentration experiments. Moreover, the washcoat loading was constraint to be within ±10% of the nominal washcoat loading provided by the vendor. The optimization is performed over the whole experimental region in order to determine the actual washcoat loading of each sample with high confidence.

The proposed algorithm and the detailed information about its implementation can be found in Supporting Information.

RESULTS

The present work aimed at characterizing the adsorption of NH_3 on a vanadium-based SCR catalyst over a wide range of conditions using the transient data obtained from a gas flow reactor. Toward this aim, we developed a comprehensive method for the processing of the experimental raw data and the removal of artifacts in order to estimate the adsorption capacity. The importance of such a method is illustrated in Figure 7 that shows the adsorption of NH_3 on the oxidized catalyst at 100 °C in the presence of 0.5% water. Panel (a) shows the adsorption capacity obtained from the unprocessed data, while panel (b) shows the processed data using the procedure developed in this work.

Two main differences between the unprocessed and the processed data are observed: the data dispersion between similar conditions and the overestimation of adsorption capacity for the unprocessed isotherms. The data dispersion is a consequence of the error propagation in time induced by signal offset effects, the lack of a flow calibration step, and the normalization by the nominal washcoat loading. Moreover, the

https://doi.org/10.1021/acs.iecr.1c01480
Ind. Eng. Chem. Res. 2021, 60, 11399−11411

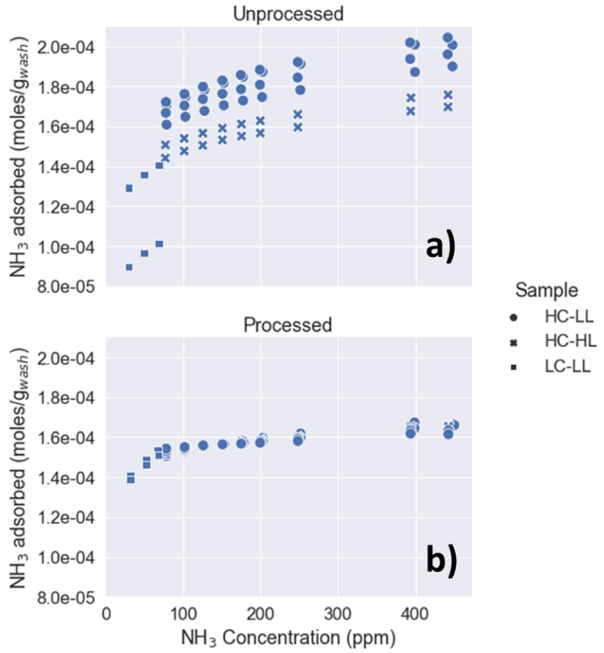

Figure 7. NH_3 adsorption isotherm at 100 °C, for the oxidized catalyst sample at 0.5% water concentration based on (a) unprocessed data and (b) processed data. Symbols refer to different catalyst samples and different feed gas concentrations: circles (HC−LL): high-concentration low-loading sample. Cross (HC−HL): high-concentration high-loading sample. Squares (LC−LL): low-concentration low-loading sample.

overestimation of the adsorption capacity in the unprocessed data is due to NH_3 adsorption in the experimental setup and dispersion and delay effects. Accounting for all these artifacts results in a continuous and monotonic increasing adsorption isotherm, as shown in Figure 7b (notice that Figure 7b shows the same experiments as Figure 7a without any averaging over the repetitions).

The adsorption isotherms obtained with the proposed data processing method over the whole experimental region are shown in Figure 8. The different panels show the isotherms for the two catalyst oxidation states (rows) and the three different water concentrations considered in this work (columns). The individual isotherms are well-separated and allow for an unambiguous characterization of the effect of temperature, oxidation state, and water content which is a direct result of the data processing method applied in this work. Specifically, Figure 8 shows the decrease in the adsorption capacity with increasing temperature and the increase with increasing NH_3 concentrations. The small increase in the adsorption isotherms in the studied range of concentration reflects the complexity of the active surface of the vanadium-based SCR catalyst where multiple, and equally distributed, adsorption sites with different natures are present.[23−25] This has been observed in different studies at the molecular scale.[25,26]

Moreover, the fully oxidized catalyst has more than 50% higher NH_3 adsorption capacity compared to the reduced catalyst. This explains the importance of the reoxidation step in the SCR mechanism, where the active sites are regenerated and the NH_3 storage capacity is restored. Furthermore, this difference in adsorption capacity strongly indicates the diversity of adsorption sites on the surface of the vanadium-based SCR catalyst, where some sites are more prone to be reduced by NH_3 at high temperature. This has been observed for the catalyst in the reduced state since the pretreatment was performed with NH_3 at 500 °C.

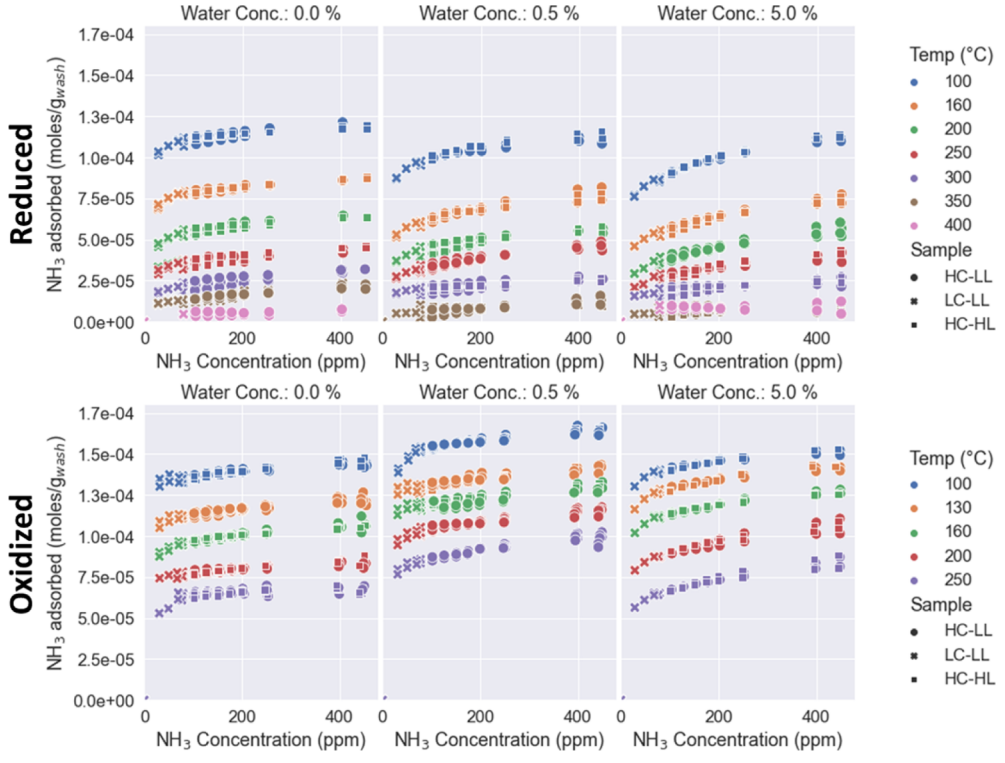

Figure 8. Adsorption isotherms for NH_3 on a vanadium-based SCR for different oxidation states of the catalyst and different water concentrations. The different symbols refer to the different catalyst samples and different feed gas concentrations (symbols have the same meaning as in Figure 7).

https://doi.org/10.1021/acs.iecr.1c01480
Ind. Eng. Chem. Res. 2021, 60, 11399−11411

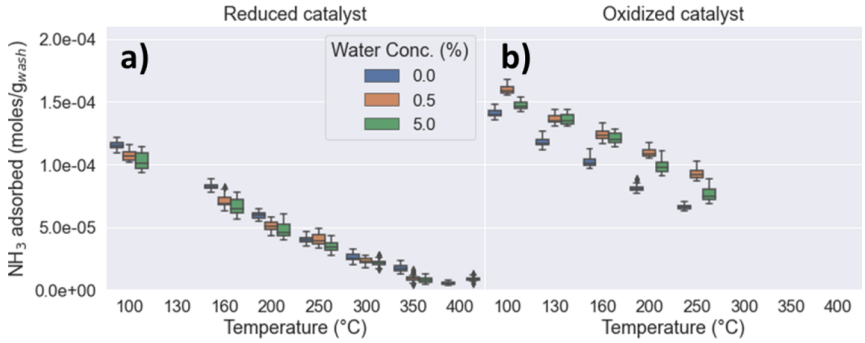

Figure 9. Average adsorption capacity for an NH_3 concentration in the range 125−400 ppm for different water concentrations and temperatures. (a) Reduced catalyst and (b) oxidized catalyst.

The water concentration has a significant effect on the NH_3 adsorption on the vanadium-based SCR catalyst. For the reduced-state catalyst, the presence of water reduces the NH_3 adsorption capacity as noticed in the decrease in the magnitude of the isotherms with increasing water concentration. However, for the oxidized catalyst, the adsorption capacity is found to exhibit a maximum at a water concentration of 0.5% independently of temperature. This behavior has also been observed in other studies, where it is explained by water dissociation and creation of new adsorption sites (Brønsted) at low concentration and water competing for adsorption sites at high concentrations.[24,26,27]

To further explore the influence of water, in Figure 9, we show the average adsorption capacity for NH_3 concentrations between 125 and 400 ppm at different temperatures and water concentrations. For the reduced catalyst, two regions can be observed: a low-temperature region (from 100 to 200 °C) where there is a considerable reduction in the NH_3 adsorption capacity when water is added and a high-temperature region (from 250 to 400 °C) where water has a negligible effect. This is an indication for an adsorption site for NH_3 with no interaction with water. On the other hand, for the oxidized catalyst, the NH_3 adsorption capacity increases when the water concentration is increased from 0 to 0.5%, while it decreases when more water is added. The gain and loss in adsorption capacity with increasing water concentration is more pronounced at higher temperatures. This can be related to an adsorption site for which the capacity is enhanced at low water concentrations, while inhibited at high water concentration. The increase in NH_3 adsorption capacity can be explained by the dissociation of water which creates new Brønsted sites on the surface of the catalyst.[25,27] Since the decline in capacity at higher temperatures is larger, this could be explained as an inhibitory effect in multiple adsorption sites.

From the obtained results, an adsorption mechanism could be proposed for model development. The mechanism should involve competitive adsorption with water, reducing the NH_3 storage capacity for the oxidized and reduced catalyst. On the other hand, it should include increased NH_3 adsorption at low water concentrations for the oxidized catalyst. Furthermore, multiple adsorption sites need to be considered on the catalyst surface.

Notice that the effect of the water concentration on the oxidized catalyst was not possible to identify from the analysis of the unprocessed data where experimental artifacts overshadow the subtle influence of water. In Supporting Information, a comparison of the data scattering between the processed and unprocessed data for the average NH_3 adsorption capacity is presented. The high dispersion for the unprocessed data gives no statistical significance for the water effect on the NH_3 adsorption capacity.

DISCUSSION

The proposed data processing method for gas flow reactors allows for obtaining data at high resolution that admit well-defined regions for NH_3 adsorption. This opens new possibilities in the data analysis of other phenomena of catalysts in gas flow reactors under transient conditions, such as reactions and regeneration, among others, since the main artifacts and effects occurring in a real reactor are characterized and better defined.

For comparison purposes, the absolute difference between the unprocessed and processed data is grouped at different variables such as temperature and NH_3 and water concentration. In Figure 10, the absolute difference at different temperatures is presented. The obtained differences have similar values for different experimental conditions, around $1-2 \times 10^{-5}$ mol/g_{wash}, because the main contribution comes from the experimental setup which was operated with the same configuration through all the experiments. The delay and

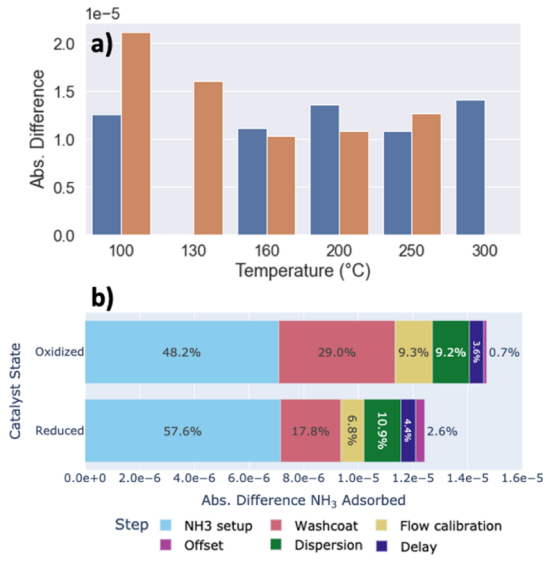

Figure 10. Preprocessing method comparison using the difference between processed and unprocessed data. (a) Absolute difference grouped by temperature. Blue bars are referred to the reduced state catalyst and orange bars are referred to the oxidized state catalyst. (b) Contribution of each preprocessing step in the magnitude difference.

https://doi.org/10.1021/acs.iecr.1c01480
Ind. Eng. Chem. Res. 2021, 60, 11399−11411

dispersion effects have almost identical values since the gas flow is constant for all the experiments and only small changes due to NH_3 concentration and temperature change are expected. Moreover, the pipelines and accessories account for most of the NH_3 adsorbed in the experimental setup and they are kept at a constant temperature (180 °C) for all the experiments. However, as the reduced state has lower NH_3 adsorption values, the overestimation by the unprocessed data will have a higher impact. This is relevant, when considering the NH_3 storage under operating conditions with NO_x reduction and reoxidation as the rate-limiting step.

Moreover, the contribution of each data processing step was evaluated on the difference magnitude between the unprocessed and processed values for NH_3 storage capacity. The contribution of each step for the reduced and oxidized catalyst sample is shown in Figure 10. Steps such as NH_3 adsorption on the experimental setup, dispersion, and delay correction have the same absolute value regarding the catalyst oxidation state since they depend on the experimental setup only. However, their relative contribution in the oxidized and reduced catalyst is different with respect to the total magnitude. The step with the highest impact in the method is the NH_3 removal from the experimental setup, followed by the washcoat uncertainty correction. The flow calibration and the delay correction step are also relevant for the method with a joined contribution of 15−20%. Furthermore, the offset correction has the lowest impact in the NH_3 storage capacity correction followed by the delay correction step. Nevertheless, these steps are important for identifying steady-state times and reference states for the flow calibration based on the FTIR measurements.

The contribution of each data processing step could be different between different experimental setups, since the NH_3 adsorbed in the experimental setup, as well as the dispersion and delay effects, depends on the experimental setup configuration, for example, pipeline length, accessories, sensor types, and so forth. However, the joint contribution of these effects, related to the experimental setup, is between 70 and 80%. As a result, the characterization of the experimental setup is a crucial stage in data processing for transient data obtained from a gas flow reactor. Furthermore, accounting for the uncertainties in the catalyst sample due to handling and production could account for an overestimation contribution of 30−20%.

Finally, in connection with the washcoat loading optimization step, the actual washcoat loadings of the different catalyst samples (284, 383, and 301 g/L for the three catalyst samples listed in Table 2) obtained from our data processing routine differ by less than 10% from the nominal washcoat loading reported by the vendor (288, 371, and 288 g/L, see Table 2). The small differences in the washcoat loading are explained by nonuniformities in the original catalyst from which the samples were prepared and sample handling during the experiment.

CONCLUSIONS

NH_3 adsorption isotherms were obtained for a vanadium-based SCR catalyst coated on a monolith substrate over a wide experimental region, where variables such as temperature, NH_3 concentration, water concentration, and catalyst oxidation state were analyzed. These were acquired with a gas flow reactor, where the gas flow is regulated by MFCs and the outlet gas phase composition is analyzed with an FTIR instrument.

The obtained NH_3 adsorption isotherms confirm the dynamic behavior of the catalyst surface, composed of multiple adsorption sites of different natures. Temperature has an important role, where the NH_3 storage capacity decreases by 50% when the adsorption temperature is increased from 100 to 250 °C. This is expected at high temperatures as the weakly adsorbed NH_3 will desorb from the catalyst surface. Moreover, the catalyst oxidation state influences the adsorption of NH_3, which strongly indicates the presence of different adsorption sites on the surface of the vanadium-based SCR catalyst, where some sites are more reduced by NH_3 at high temperatures. The reduction of the catalyst is a reversible process, where the catalyst can be reoxidized and restore its full capacity when it is exposed to oxygen. Additionally, water has a complex effect on the NH_3 adsorption as it can increase the NH_3 storage capacity at low water concentrations when the catalyst is oxidized and at the same time can inhibit NH_3 adsorption at high concentrations. For the catalyst in the reduced state, water decreases the NH_3 storage capacity in most of the cases.

Using a gas flow reactor for such experiments required the development of a data processing method, characterizing the gas flow reactor as a real reactor and identifying artifacts. The proposed method involves the characterization of delay and dispersion effects using an RTD model and the identification of artifacts such as NH_3 adsorbed in the experimental setup and washcoat uncertainties.

Furthermore, with the aid of this method, the effects on the identified artifacts were removed, which could account for 15−125% of the NH_3 adsorption values. The effect of such artifacts is higher at higher temperatures where the NH_3 storage capacity is lower. The requirement for accuracy at high temperatures is more demanding as lower NH_3 adsorption values are prone to be more affected by artifacts, and high-temperature adsorption data are relevant in the vehicles' operating region.

Additionally, the proposed normalization by the washcoat loading with the optimization step for dealing with uncertainties gives the possibility to integrate different data sets from different samples. The obtained isotherms, integrating diverse catalyst samples, exhibit continuous and monotonic increasing behavior. This will make data from different samples comparable and it will increase the sample size with independent observations. As a result, the experimental region is expanded.

The obtained data set from transient data identifying steady-state steps is an alternative for avoiding microreactor experiments and to complement TPD measurement results. The proposed method provides high resolution, shown by the low data spread and the well-defined regions for adsorption. Therefore, the obtained data set from this method could improve the model parameter estimation since the main effects in a real reactor were characterized using an RTD model, and the identified artifacts were removed with a systematic method using the different processing steps which have been justified experimentally in this study. Finally, the proposed method could be extended to other adsorbates or other transient data analysis in a catalyst such as reaction or regeneration rates.

ASSOCIATED CONTENT

Supporting Information

The Supporting Information is available free of charge at https://pubs.acs.org/doi/10.1021/acs.iecr.1c01480.

Detailed description of the proposed data processing method (PDF).

https://doi.org/10.1021/acs.iecr.1c01480
Ind. Eng. Chem. Res. 2021, 60, 11399−11411

AUTHOR INFORMATION

Corresponding Author

Andres F. Suarez-Corredor − *Competence Centre for Catalysis, Chalmers University of Technology, Gothenburg 412 96, Sweden; Scania CV AB, Södertälje 151 87, Sweden;* orcid.org/0000-0002-6112-0183; Email: andres.suarez@scania.com

Authors

Matthäus U. Bäbler − *Department of Chemical Engineering, KTH Royal Institute of Technology, Stockholm 100 44, Sweden;* orcid.org/0000-0001-7995-3151

Louise Olsson − *Competence Centre for Catalysis, Chalmers University of Technology, Gothenburg 412 96, Sweden;* orcid.org/0000-0002-8308-0784

Magnus Skoglundh − *Competence Centre for Catalysis, Chalmers University of Technology, Gothenburg 412 96, Sweden;* orcid.org/0000-0001-7946-7137

Björn Westerberg − *Scania CV AB, Södertälje 151 87, Sweden*

Complete contact information is available at: https://pubs.acs.org/10.1021/acs.iecr.1c01480

Notes

The authors declare no competing financial interest.

ACKNOWLEDGMENTS

This research project is sponsored by Scania CV AB. The Competence Centre for Catalysis is hosted by Chalmers University of Technology and financially supported by the Swedish Energy Agency and the member companies AB Volvo, ECAPS AB, Johnson Matthey AB, Preem AB, Scania CV AB, Umicore Denmark ApS, and Volvo Car Corporation AB. The authors acknowledge Umicore for providing the catalyst samples.

NOMENCLATURE

Notation

Δt	time step (s)
ρ_{WC}	washcoat loading (g/L)
τ_1	time scale parameter for delay effects (s)
τ_2	time scale parameter for dispersion effects (s)
F	molar flow (mol/s)
f_{dis}	low-pass filter parameter for dispersion correction
N	normalized accumulation by washcoat loading (moles/g_{wash})
n	adsorbed amount over catalyst (moles)
P	pressure (Pa)
q	volumetric flow (NL/min)
T	temperature (K)
t	time (s)
V_s	sample volume (L)
y	gas composition (ppm)

Subscripts

c	compensated value
del	delay processed value
exp	experimental setup
FTIR	value from FTIR
i	index of time
int	interval
MFC	value from MFCs
ref	reference value
Tot	total value

REFERENCES

(1) Heck, R. M.; Farrauto, R. J.; Gulati, S. T. *Catalytic Air Pollution Control: Commercial Technology*; John Wiley & Sons, 2016.

(2) Frey, H. C. Trends in onroad transportation energy and emissions. *J. Air Waste Manage. Assoc.* **2018**, *68*, 514−563.

(3) Senecal, P. K.; Leach, F. Diversity in transportation: Why a mix of propulsion technologies is the way forward for the future fleet. *Results Eng.* **2019**, *4*, 100060.

(4) Sauer, J.; Freund, H.-J. Models in catalysis. *Catal. Lett.* **2015**, *145*, 109−125.

(5) Ertl, G. Reactions at surfaces: From atoms to complexity (Nobel lecture). *Angew. Chem., Int. Ed.* **2008**, *47*, 3524−3535.

(6) Nova, I.; Tronconi, E. *Urea-SCR Technology for deNOx after Treatment of Diesel Exhausts*; Springer, 2014; Vol. *5*.

(7) Metkar, P. S.; Salazar, N.; Muncrief, R.; Balakotaiah, V.; Harold, M. P. Selective catalytic reduction of NO with NH3 on iron zeolite monolithic catalysts: Steady-state and transient kinetics. *Appl. Catal., B* **2011**, *104*, 110−126.

(8) Tronconi, E.; Nova, I.; Ciardelli, C.; Chatterjee, D.; Bandl-Konrad, B.; Burkhardt, T. Modelling of an SCR catalytic converter for diesel exhaust after treatment: Dynamic effects at low temperature. *Catal. Today* **2005**, *105*, 529−536.

(9) Chatterjee, D.; Burkhardt, T.; Bandl-Konrad, B.; Braun, T.; Tronconi, E.; Nova, I.; Ciardelli, C. Numerical simulation of ammonia SCR-catalytic converters: model development and application. *SAE Trans.* **2005**, *114*, 437−448.

(10) Olsson, L.; Wijayanti, K.; Leistner, K.; Kumar, A.; Joshi, S. Y.; Kamasamudram, K.; Currier, N. W.; Yezerets, A. A multi-site kinetic model for NH3-SCR over Cu/SSZ-13. *Appl. Catal., B* **2015**, *174−175*, 212−224.

(11) Nova, I.; Ciardelli, C.; Tronconi, E.; Chatterjee, D.; Bandl-Konrad, B. NH3-SCR of NO over a V-based catalyst: Low-T redox kinetics with NH3 inhibition. *AIChE J.* **2006**, *52*, 3222−3233.

(12) Sjövall, H.; Blint, R. J.; Olsson, L. Detailed kinetic modeling of NH3 SCR over Cu-ZSM-5. *Appl. Catal., B* **2009**, *92*, 138−153.

(13) Åberg, A.; Hansen, T. K.; Linde, K.; Nielsen, A. K.; Damborg, R.; Widd, A.; Abildskov, J.; Jensen, A. D.; Huusom, J. K. A Framework for Modular Modeling of the Diesel Engine Exhaust Gas Cleaning System. *Comput.-Aided Chem. Eng.* **2015**, *37*, 455−460.

(14) Åberg, A.; Widd, A.; Abildskov, J.; Huusom, J. K. Parameter estimation and analysis of an automotive heavy-duty SCR catalyst model. *Chem. Eng. Sci.* **2017**, *161*, 167−177.

(15) Christiansen, T.; Jensen, J.; Åberg, A.; Abildskov, J.; Huusom, J. Methodology for developing a diesel exhaust after treatment simulation tool. *SAE Int. J. Commer. Veh.* **2017**, *11*, 45−56.

(16) Ciardelli, C.; Nova, I.; Tronconi, E.; Konrad, B.; Chatterjee, D.; Ecke, K.; Weibel, M. SCR-DeNOx for diesel engine exhaust aftertreatment: unsteady-state kinetic study and monolith reactor modelling. *Chem. Eng. Sci.* **2004**, *59*, 5301−5309.

(17) Levenspiel, O.; Bischoff, K. B. Patterns of flow in chemical process vessels. *Adv. Chem. Eng.* **1964**, *4*, 95−198.

(18) Levenspiel, O. *Chemical Reaction Engineering*; John Wiley & Sons, 1999.

(19) Draper, N. R.; Smith, H. *Applied Regression Analysis*; John Wiley & Sons, 2014; Vol. *326*.

(20) Griva, I.; Nash, S. G.; Sofer, A. *Linear and Nonlinear Optimization*; Siam, 2009; Vol. *108*.

(21) Zhdanov, V. P.; Pavlíček, J.; Knor, Z. Preexponential factors for elementary surface processes. *Catal. Rev.: Sci. Eng.* **1988**, *30*, 501−517.

(22) Kolb, W. B.; Papadimitriou, A.; Cerro, R.; Leavitt, D.; Summers, J. The ins and outs of coating monolithic structures. *Chem. Eng. Prog.* **1993**, *89*, 63−67.

(23) Marberger, A.; Ferri, D.; Elsener, M.; Kröcher, O. The Significance of Lewis Acid Sites for the Selective Catalytic Reduction of Nitric Oxide on Vanadium-Based Catalysts. *Angew. Chem., Int. Ed.* **2016**, *55*, 11989−11994.

(24) Zhao, Z.; Li, E.; Qin, Y.; Liu, X.; Zou, Y.; Wu, H.; Zhu, T. Density functional theory (DFT) studies of vanadium-titanium based selective catalytic reduction (SCR) catalysts. *J. Environ. Sci.* **2020**, *90*, 119−137.
(25) Topsøe, N.-Y.; Anstrom, M.; Dumesic, J. Raman, FTIR and theoretical evidence for dynamic structural rearrangements of vanadia/titania DeNOx catalysts. *Catal. Lett.* **2001**, *76*, 11−20.
(26) Topsoe, N. Y.; Dumesic, J. A.; Topsoe, H. Vanadia-titania catalysts for selective catalytic reduction of nitric-oxide by ammonia: II Studies of active sites and formulation of catalytic cycles. *J. Catal.* **1995**, *151*, 241−252.
(27) Wachs, I. E.; Weckhuysen, B. M. Structure and reactivity of surface vanadium oxide species on oxide supports. *Appl. Catal., A* **1997**, *157*, 67−90.

https://doi.org/10.1021/acs.iecr.1c01480
Ind. Eng. Chem. Res. 2021, 60, 11399−11411